

Probabilistic Seismic Hazard Assessment of the Meers Fault, Southwestern Oklahoma: Modeling and Uncertainties

Emma M. Baker and Austin A. Holland



Special Publication
SP2013-02

DRAFT REPORT
MAY 16, 2013

OKLAHOMA GEOLOGICAL SURVEY
Sarkeys Energy Center
100 East Boyd St., Rm. N-131
Norman, Oklahoma 73019-0628

SPECIAL PUBLICATION SERIES

The Oklahoma Geological Survey's Special Publication series is designed to bring new geologic information to the public in a manner efficient in both time and cost. The material undergoes a minimum of editing and is published for the most part as a final, author-prepared report.

Each publication is numbered according to the year in which it was published and the order of its publication within that year. Gaps in the series occur when a publication has gone out of print or when no applicable publications were issued in that year.

This publication is issued by the Oklahoma Geological Survey as authorized by Title 70, Oklahoma Statutes, 1971, Section 3310, and Title 74, Oklahoma Statutes, 1971, Sections 231-238.

This publication is only available as an electronic publication.

1. Table of Contents

2. Summary	4
3. Introduction.....	5
3.1. Geologic Background	7
3.2. Structure of the Meers Fault.....	7
3.3. Previous Studies of the Meers Fault.....	7
4. Meers Fault PSHA Parameters and Methods.....	8
4.1. Recurrence Interval for the Meers Fault.....	8
4.2. Magnitude and A-Value Calculation	8
4.3. Dip and Rake.....	9
4.4. Additional PSHA Parameters and Methods.....	9
5. PSHA Results	10
5.1. Peak Ground Acceleration (PGA) Simulation Results.....	10
6. Discussion and Conclusions.....	13
7. Acknowledgements	16
8. References	16

2. Summary

The Meers fault located in southwestern Oklahoma is the only known Holocene fault with a surface expression in Oklahoma. Since the movement on the fault did not occur in the historical record, the hazards associated with the Meers fault are not well understood. Using OpenQuake software and the OpenSHA platform, a Probabilistic Seismic Hazards Assessment (PSHA) was determined by 25 Monte Carlo traverses through three-branches of a probabilistic logic-tree. The Peak Ground Acceleration (PGA) was modeled to observe the effect of certain parameters on the hazards associated with the fault. Some of the parameters evaluated include the recurrence interval, rupture length, dip and rake. Recurrence intervals of 1,300, 4,500, 20,000 and 100,000 years were obtained from the published literature. Magnitude of a potential earthquake was calculated based on the rupture length. Rupture lengths were measured using aerial photographs and the United States Geological Survey (USGS) Quaternary fault database. The magnitudes obtained for a rupture length of 58.21 km were M7.10 and M7.11 for strike-slip and reverse/thrust motion, respectively. The magnitudes for a length of 30.08 km were M6.82 and M6.80 for strike-slip and reverse/thrust motion, respectively. The a-values were then calculated for each recurrence interval and assigned to different recurrence scenarios with the PSHA. Dip values of 70° and 55° were used based on previous studies of the Meers fault. The rake values used in the study were 30° and 11°. Since the recurrence interval of 4,500 years had an a-value similar to the current Oklahoma a-values, the PSHA for sensitivity to dip and rake scenarios were run using only 4,500 years. Other parameters such as the attenuation models and probability of exceedance (POE) were consistent throughout the study. Although all of the parameters had an effect on the PGA, the most prominent effect was from the recurrence interval. The recurrence interval between major earthquakes on the Meers fault has large uncertainties and has the most dramatic affect on the estimated ground motion within the PSHA. Future work is needed to better constrain the recurrence interval on the Meers fault. The results of this study were about twice as large as the values achieved through the USGS National Seismic Hazard (NSH) study conducted in 2008. The results obtained in this study are theoretical and contain uncertainty; they should not be used in real world application. The difference in the results indicates the need for further research to reduce the uncertainty in PSHA and to the fully understand the effect of certain parameters on the hazards assessment.

3. Introduction

The Meers fault is located in southwest Oklahoma. It represents the only known Oklahoma Holocene faulting with a surface rupture. As such, it is important to fully understand the hazard associated with this fault. A great deal of uncertainty remains about many significant parameters required to quantify the seismic hazard associated with the Meers fault. This paper addresses the impact these uncertainties have on Probabilistic Seismic Hazard Assessments (PSHA) of the Meers fault and clearly demonstrates the need for more research to reduce these uncertainties. We will examine information in the published literature that characterizes the Meers fault in the context of a PSHA determination. We compare PSHA results using different characterizations of the Meers fault and indicate which uncertainties lead to obscuring the PSHA results.

The probabilistic seismic hazard assessment (PSHA) calculations were determined using newly available open-source software called OpenQuake version 0.7.0 released May 10, 2012 (Crowley et al., 2012; Field et al., 2003). Using the OpenSHA (Field et al., 2003) platform, the PSHA is determined by conducting multiple Monte Carlo traverses of a probabilistic logic-tree. For all cases, 25 traverses of the logic tree were conducted. The three branches of the logic tree used in the calculations were as follows (see Table 3):

1. Description of the earthquake source models,
2. Describes the maximum magnitude probabilities for the earthquake sources, and
3. The ground motion prediction equations (GMPE).

The fault is located in southwestern Oklahoma in Comanche and Kiowa counties (Figure 1). Due to the lack of movement in the historic record, very little work has been done to update the possible hazards associated with the Meers fault. The last time the Meers fault had a major rupture was approximately 1,300 years ago. The magnitude estimate ranges from 6.0 to greater than 7.0. The hazards assessment done by organizations such as the United States Geological Survey (USGS) may not fully capture the possible magnitudes and ground motions that the Meers fault could generate. The national hazard map by the USGS (Peterson et al., 2008) has a single recurrence interval of 4,500 years. A single recurrence interval may not represent the potential range for the Meers fault. The Oklahoma Geological Survey (OGS) re-evaluated of the potential size of an earthquake that could occur along the fault. With help from newly available digitally imagery, the possible surface rupture length was re-evaluated. The OGS presents an up-to-date assessment of the Meers fault using a full range of variables and updated information to obtain a more accurate picture of the hazards associated with the fault. Since only the Meers fault is considered in this study, the ground-motion prediction results are not intended for seismic design calculations.

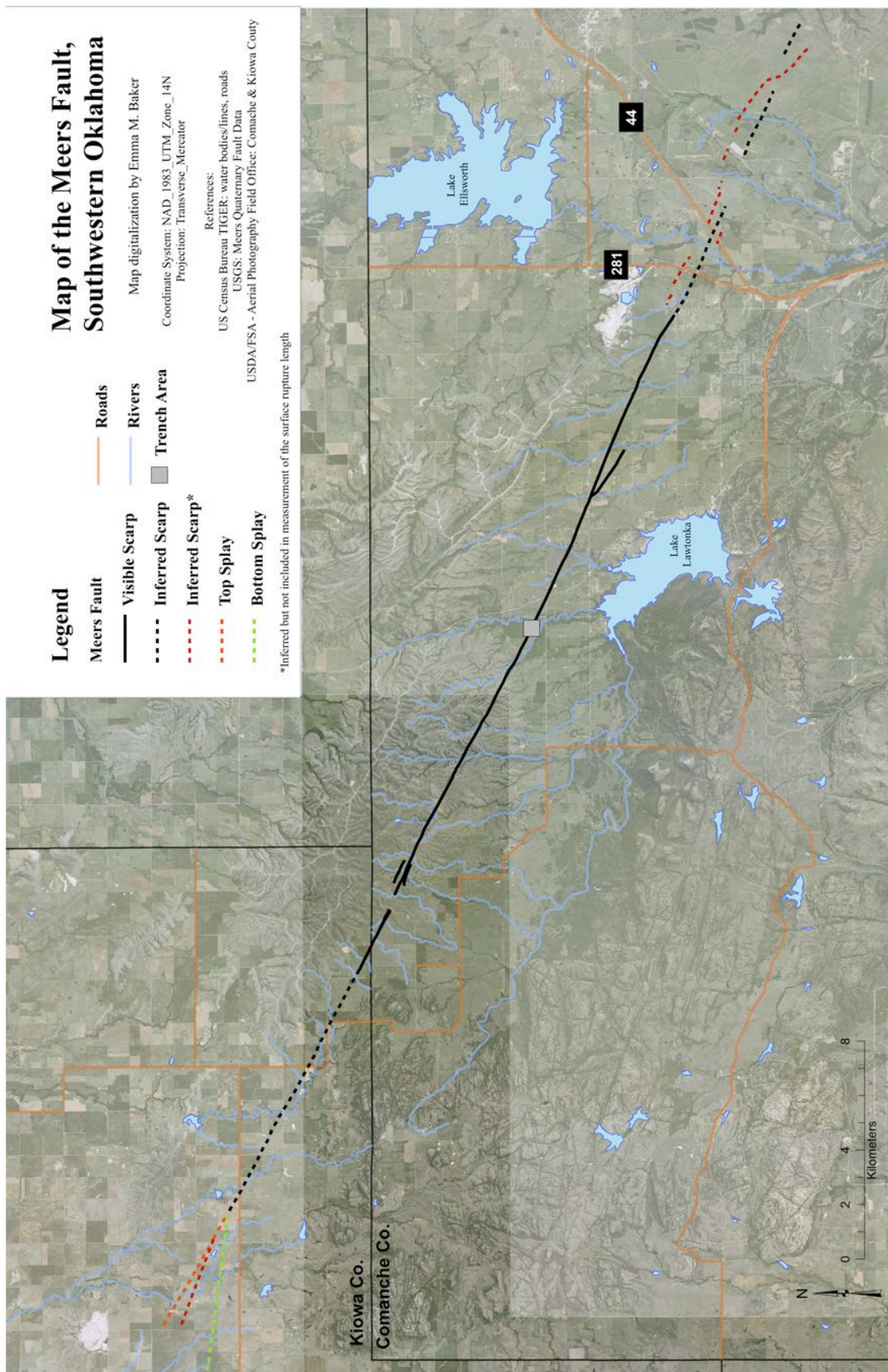


Figure 1. Map of the fault segments for the Meers Fault in SW Oklahoma. Surface rupture definitions shown for the Meers fault are from (USGS, 1994).

3.1. Geologic Background

The Meers fault is part of the Wichita Frontal Fault (WFF) system, which separates the Anadarko-Ardmore basin to the northeast and the Wichita-Amarillo uplift to the southwest (Harlton, 1963). The WFF system extends about 175 km across southern Oklahoma and parts of the Texas Panhandle (Ham et al., 1964; Harlton, 1963). Between the late Precambrian and early Cambrian (~540 Ma), an early stage of rifting occurred and produced igneous body intrusions and basaltic flows in addition to normal faulting (Crone and Luza, 1990; Luza et al., 1987). From the late Cambrian to late Mississippian, subsidence of the Anadarko basin began with mostly carbonate sediments with some clastic units (Crone and Luza, 1990; Luza et al., 1987). Sedimentation during this time period produced over 3 km thick deposits near the basin's deepest part (Luza et al., 1987). In the early Pennsylvanian to Permian, the tectonically active area experienced block faulting, uplift and syntectonic sedimentation to form a deep basin over 7.5 km (Luza et al., 1987). Due to crustal weaknesses from the Cambrian, the uplift caused transpressional left-lateral movement to occur along the fault (Crone and Luza, 1990; Luza et al., 1987). The displacement and throw of the fault are difficult to determine and, therefore, unknown (Crone and Luza, 1990).

The Meers fault displaces Holocene sediments at the surface indicating a recent movement. Any movement in the post-Paleozoic is difficult to determine because of the lack of Permian rocks in the exposures (Crone and Luza, 1990). The oldest evidence in the Quaternary occurs as offset in valleys and ridges in the middle to late Pleistocene sediments (Jones-Cecil, 1995; Luza et al., 1987). The displaced alluvium deposits coupled with carbon (C^{14}) dating indicates the fault displaces all units except the youngest, East Cache Alluvium (Crone and Luza, 1990; Luza et al., 1987; Madole, 1988). The C^{14} dating has suggested that the most recent scarp movement occurred about 1,700-1,300 years ago (Luza et al., 1987).

3.2. Structure of the Meers Fault

The regional horizontal compressive stress for the Central North America is known to be NE to ENE (Zoback and Zoback, 1980; Hermann et al., 2011). This favors left-lateral movement on WNW faults like the Meers fault (Crone and Luza, 1990). During the Paleozoic, the faulting occurred down to the north with an estimated slip of 2 km (Jones-Cecil, 1995; Crone and Luza, 1990). The Holocene fault movement was down to the south with a left-lateral slip component (Jones-Cecil 1995; Crone and Luza, 1990). Near the northwestern end of the fault, splaying appears to have occurred which would be geometrically consistent with rupture propagation barriers (Jones-Cecil, 1995). This may have terminated the ruptures during either one or both Holocene movements. The secondary faults on the southeastern end on the scarp are not apparent in ground-magnetic profiles due to primarily strike-slip faulting or limited to a non-magnetic sedimentary section (Jones-Cecil, 1995).

The scarp trends N60°W. Estimates for the rupture length of the Meers fault vary significantly. The original estimate of 26 km was based on the length of scarp apparent in the bedrock geology (Luza et al., 1987; Crone and Luza, 1990). However, in low-angle sun aerial photograph of the southeastern extension, the surface rupture length was revised to about 37 km (Ramelli and Slemmons, 1986). Based on the geophysical expression, the rupture length in the subsurface could be as long as 70 km (Slemmons et al., 1980). Using measurements taken from the digital imagery, the visible scarp extends approximately 30.1 km (Figure 1). The USGS Quaternary fault database (USGS, 1994) gives inferred scarp to the northwest up to the splaying is about 11.5 km, and the inferred scarp to the southeast is about 6.9 km. The total length from the southeast end to the top splay (4.9 km) is roughly 53.3 km. The length of the bottom splay was measured at 5.8 km and used as a continuation on the linear path of the well-expressed scarp to get a total length of 54.3 km.

3.3. Previous Studies of the Meers Fault

In a previous study, two trenches were dug across the fault to determine the sense of motion and

timing of the earthquakes on the Meers fault (Crone and Luza, 1990). The trench area on the map in Figure 1 is the general location of the two trenches. The first trench is located about 150 m ESE of Canyon Creek and the second is located approximately 200 m ESE of trench 1.

Trench 1 was 22 m long and about 2.5 m deep (Crone and Luza, 1990). The dimensions of the scarp in this area were roughly 2.4 m high with an estimated minimum surface offset of 2.2 m and a maximum slope angle of $9^{\circ}22'$. There was clear faulting in through the Hennessey Shale near the bottom of the trench and the Browns Creek Alluvium (early to middle Holocene). The alluvium was warped into a monocline over the fault movement. This implies that the scarp never had a large free face, but there are strong stratigraphic relationships indicating a surface-rupture event (Crone and Luza, 1990). There was 2 m of brittle deformation near the center of the scarp with secondary faulting probably in response to the warping. The southwest side of the fault is reverse separation and near-surface compression due to the monocline. On the northeast side, the normal separation was due to extension. There was less than 1 m of displacement for both secondary faults (Crone and Luza, 1990).

Trench 2 was 19 m long (Crone and Luza, 1990). Due to a high water table, the deepening of the trench was limited, so the bedrock on the downthrown side of fault could not be exposed any further. The scarp was about 3.4 m high with a surface offset of 3.0 m and a maximum slope angle of 9° . The fault strikes $N64^{\circ}W$, and dips $56^{\circ}NE$. The bedrock consisted of the Hennessey shale and dolomite, which was adjacent to the fault on the upthrown side. The Porter Hill Alluvium of Pleistocene age was clearly faulted. The stratigraphic throw in the trench was measured at a minimum value of 3.2 to 3.3 m. The warping of the bedforms accounts for 70% to 85% of the deformation at trench 2, and the brittle fracturing is more prominent as compared to trench 1 (Crone and Luza, 1990).

Within surficial deposits mapped in trenches, the Meers fault can be seen to have varying dip angles. However, from geophysical data the dip of the Meers fault at depth appears to be quite steep between vertical and 70° (Jones-Cecil, 1995). Estimates of the ratio of strike-slip motion to reverse vertical motion on the fault vary, but generally are on the order of about 1.3-1.5 (Crone and Luza, 1990; Kelson and Swan, 1990) consistent with a rake between 35° and 40° (Kelson and Swan, 1990).

4. Meers Fault PSHA Parameters and Methods

4.1. Recurrence Interval for the Meers Fault

The Meers fault has been largely aseismic since modern seismic monitoring has occurred in Oklahoma (1978), which creates difficulties assessing recurrence rates using modern seismicity. The last major earthquake with surface rupture known to have occurred on the Meers Fault was between 800 and 1,600 years before present (B.P.) (Crone and Luza, 1990; Kelson and Swan, 1990; Luza et al., 1987; Madole, 1988) with a preferred value of 1280 ± 140 years B.P. (Crone and Luza, 1990). Recurrence estimates range from 100,000 years (Crone and Luza, 1990) to about 1,300 years (Kelson and Swan, 1990). These varying values have very different implications to seismic hazard and demonstrate the need for further work to constrain recurrence intervals more rigorously. Due to the large variance of values in the literature and the lack of seismic evidence in recent historical time, we can only estimate the recurrence interval of the fault. The CEUS-SSC (2011) considered the short recurrence interval to occur within a cluster with an interval to be 2,153-2,968 years. In this study, we consider the hazard for recurrence intervals of 1,300, 4,500, 20,000 and 100,000 years to examine the sensitivity earthquake hazards for the Meers fault assuming different recurrence intervals.

4.2. Magnitude and A-Value Calculation

The magnitude for the Meers fault was calculated for a given rupture length. The magnitudes were inferred based on the relationship between magnitude and rupture length had an uncertainty of less than ± 0.5 for all rupture lengths. With a rupture length on the Meers fault of 53.21 km, the magnitude for strike-slip motion along the fault was $M7.10$, and the magnitude for reverse/thrust

motion was approximately the same at M7.11. A rupture length of 53.21 km is the estimated length of the visible scarp, inferred scarp and the top splay (Figure 1). A rupture length of 30.08 km on the Meers fault returned a M6.82 for strike-slip motion and a M6.80 for reverse/thrust motion. 30.08 km is the approximate length of just the visible scarp (Figure 1). The rupture length scaling relationship of Wells and Coppersmith (1994) allowed us to infer Gutenberg-Richter a-values (Gutenberg and Richter, 1944) assuming a b-value of 1.0 for our different recurrence intervals. The a-values for the rupture length 53.21 km for strike-slip and reverse/thrust motion are shown in Table 1. The a-values with a rupture length of 30.08 km on the Meers fault are shown in Table 2. Since the a-value for a recurrence interval of 4,500 years is most similar to that of the observed de-clustered OGS earthquake catalog (Holland et al., 2013). 4,500 years is the only recurrence interval considered for the reverse/thrust scenario. A recurrence of 1,300 years was consistent with the rates of de-clustered seismicity observed from 2009 through 2012. In this period, there was a significant rate increase in seismicity within Oklahoma. From the de-clustered catalog of 1882-2008, the recurrence rate of 20,000 years has a slightly lower but still comparable a-value. To fully capture the estimates made in the published literature, a longer recurrence interval of 100,000 years was included even though the a-value is lower than the normal value for Oklahoma.

Table 1. *Inferred Gutenberg-Richter a-values for different recurrence intervals of rupture length 53.21 km on the Meers Fault assuming a b-value of 1.0.*

Recurrence Interval (yrs)	a-value for Strike-slip (M7.10)	a-value for Reverse/Thrust (M7.11)
1,300	3.9861	-
4,500	3.4468	3.4568
20,000	2.7990	-
100,000	2.0100	-

Table 2. *Inferred Gutenberg-Richter a-values for different recurrence intervals of rupture length 30.08 km on the Meers Fault assuming a b-value of 1.0.*

Recurrence Interval (yrs)	a-value for Strike-slip (M6.82)	a-value for Reverse/Thrust (M6.80)
1,300	3.7061	-
4,500	3.1668	3.1468
20,000	2.5190	-
100,000	1.8200	-

4.3. Dip and Rake

The motion of the Meers fault is thought to be nearly pure strike-slip, so the dip is assumed to be very steep at about 90° according to previous studies (Crone and Luza, 1990; Jones-Cecil, 1995; Kelson and Swan, 1990; Luza et al., 1987; Madole, 1988). However, some reprocessed deep seismic reflection data suggests a slightly more shallow dip of around 70° (Jones-Cecil, 1995; Lemiszki and Brown, 1988). In addition, a dip of 55° was included in the study to account for the fault dip seen in trench 2. Two rakes were considered in the study. A rake of 30° for the fault was calculated for lateral movement twice the vertical movement, and a rake of 11° was calculated for lateral movement five times the vertical movement.

4.4. Additional PSHA Parameters and Methods

The additional parameters for this PSHA study remained constant throughout all the simulations

and are shown in Table 3. A simple fault geometry was used with a Sadigh et al. (1997) site type of rock. The probability of exceedance (POE) for this PSHA study was set to 0.02 (2%) in an investigation time of 50 years. The upper and lower seismogenic depths were set to 2.0 km and 15.0 km, respectively. The maximum and minimum magnitudes were 7.5 and 4.5 with a fault rupture offset of 5 km. The Ground Motion Prediction Equation (GMPE) branch of the logic tree gave equal weights of 0.25 (25%) to four attenuation models: Boore and Atkinson (2008), Abrahamson and Silva (2008), Chiou and Youngs (2008) and Campbell and Bozorgnia (2008). There is a 25% likelihood of a particular attenuation model occurring. Sample iteration began with picking a random source point within the defined locations along fault rupture length. One of the four attenuation models is then randomly selected to calculate the vibration of the ground from the source point for each point within the defined location. The maximum Peak Ground Acceleration (PGA) values were stored, and the next iteration began until all iterations were completed. After all the iterations were completed, the maximum PGA values were put into a storage file for later analysis. Due to some unrecognized issue with the fault specifications, we could only run 25 iterations per simulation. Generally, more iterations are required to capture all possibilities for in the PSHA analysis. Since we are conducting a sensitivity analysis of input parameters and not calculating a final PSHA for design purposes, the authors did not feel that the limited number of iterations dramatically impacted out results.

Table 3. *Additional PSHA Parameters for the Meers Fault. Sources: ¹Sadign et al. (1997)*

Parameter	Value(s)
Attenuation Models (weight for each: 0.25)	Boore and Atkinson (2008), Abrahamson and Silva (2008), Chiou and Youngs (2008), Campbell and Bozorgnia (2008)
Fault Geometry	Simple
Sadign ¹ Site Type	Rock
POE	0.02
Investigation Time	50 years
Upper Seismogenic Depth	2 km
Lower Seismogenic Depth	15 km
Maximum Magnitude	7.5
Minimum Magnitude	4.5
Fault Rupture Offset	5 km
Number of Iterations	25

5. PSHA Results

5.1. Peak Ground Acceleration (PGA) Simulation Results

Using OpenQuake software, Peak Ground Acceleration (PGA) maps displayed the estimated acceleration at the surface near and surrounding the Meers fault. Strike-slip scenarios on the Meers fault of M7.1 and M6.82 were conducted for the recurrence intervals of 1,300, 4,500, 20,000 and 100,000 years using a dip of 90° and a rake of 0° (Figure 2). Since the scale bars for each mapped scenario are different, tables with the values for the maximum PGA of each scenario were created for an easier first-glance comparison. The maximum PGA values for strike-slip motion on the Meers fault for all eight scenarios are shown in Table 4. Reverse/thrust scenarios were run using dips of 70° and 55° and rakes of 30° and 11° with a recurrence interval of 4,500 years (Figure 3). The maximum PGA values for the reverse/thrust motion are displayed in Tables 5 and 6.

PGA Maps for the Meers Fault

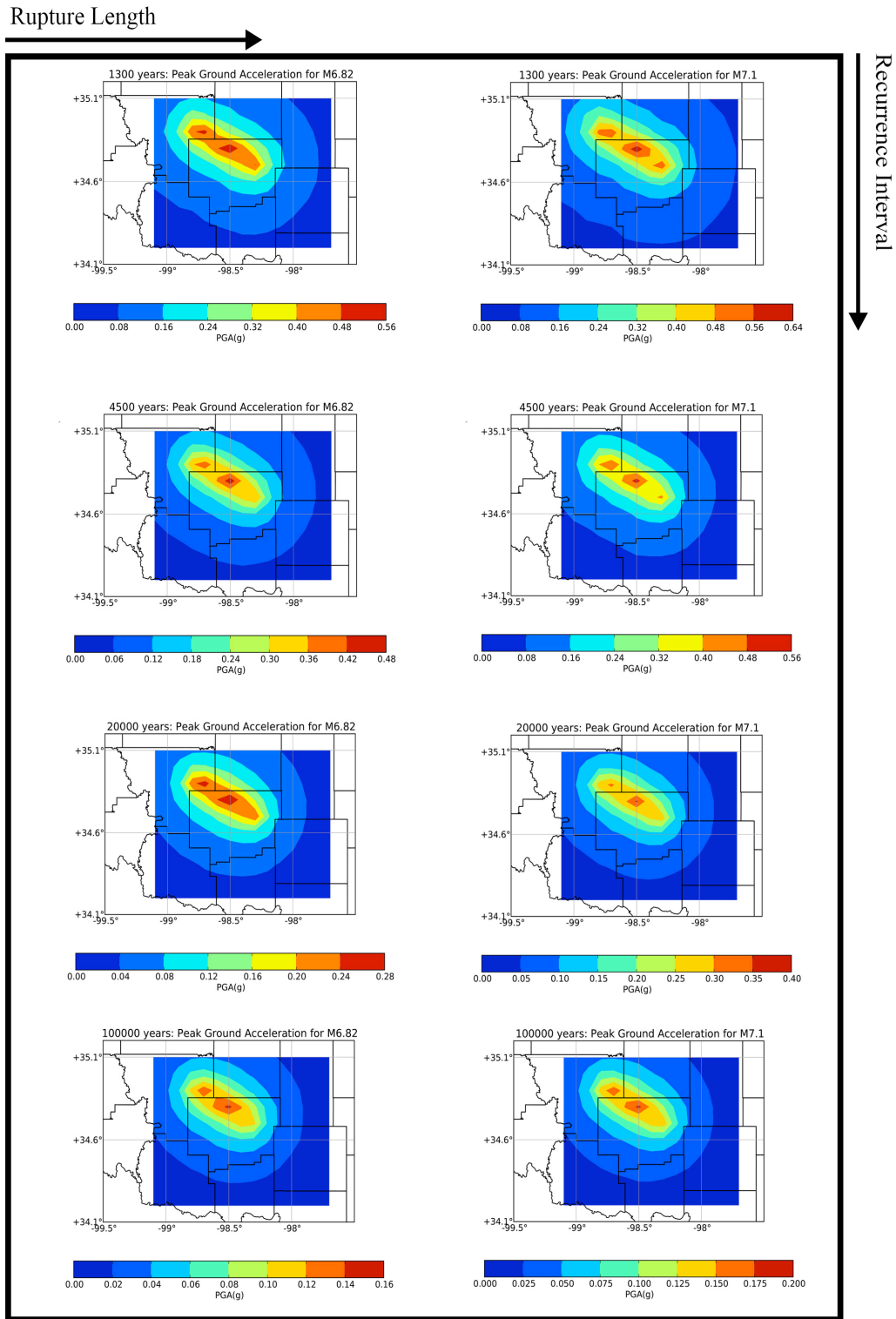


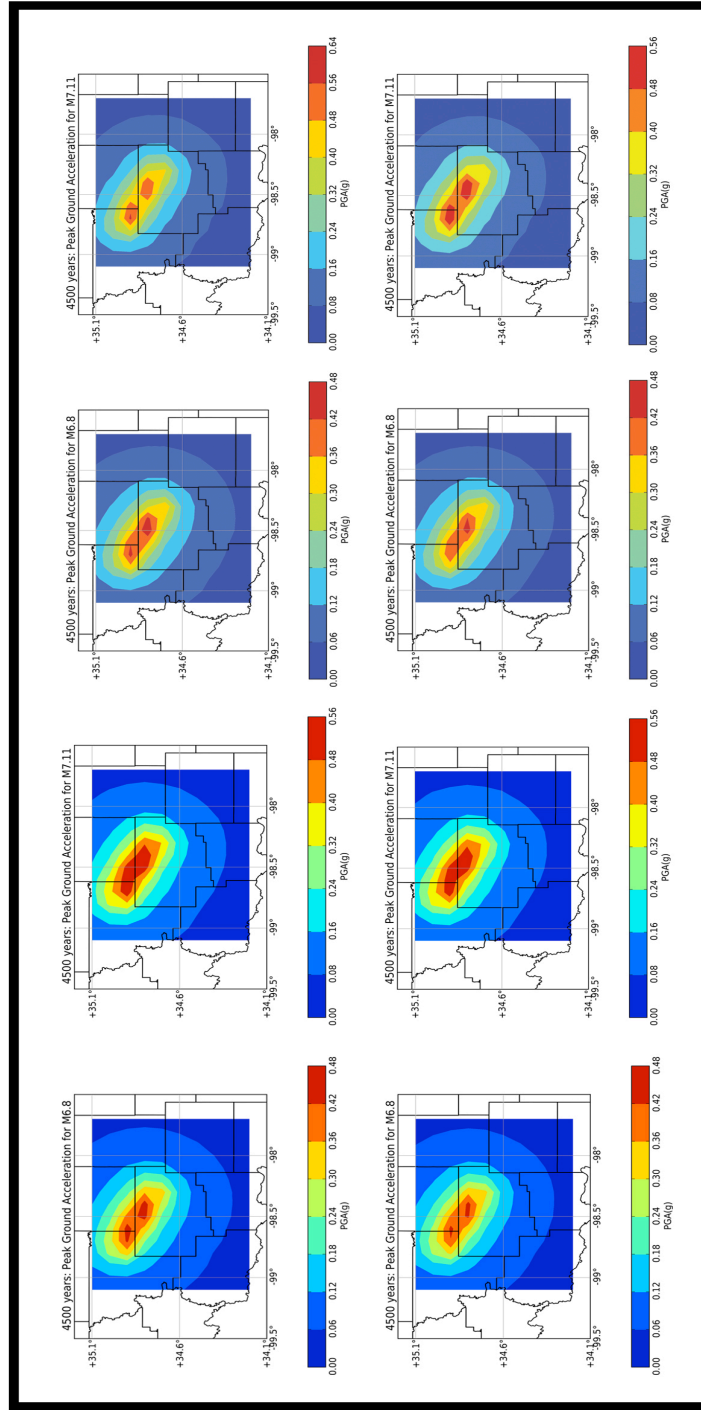
Figure 2. Peak Ground Acceleration (PGA) maps displaying changes in the ground acceleration between rupture lengths 53.21 km and 30.08 km and changes between recurrence intervals 1,300, 4,500, 20,000, 100,000 years for a strike-slip motion on the Meers fault. Note: The PGA (g) scale bars for each map are different.

PGA Maps of Dip and Rake Comparison for the Meers Fault

Recurrence Interval: 4500 years

Dip: 55°

Dip: 70°



Rake: 30°
(Rev. 1:2)

Rake: 11°
(Rev. 1:5)

Figure 3. Peak Ground Acceleration (PGA) maps displaying changes in the ground acceleration between dips of 55° and 70° and changes between rakes of 30° and 11° for a recurrence interval of 4,500 years on the Meers fault. Note: The PGA (g) scale bars for each map are different.

Table 4. Maximum Peak Ground Acceleration (PGA) (g) for **Strike-slip motion** on the Meers Fault with a **dip of 90° and rake of 0°**.

Recurrence Interval (yrs)	Max PGA (g) for Strike-slip (M7.1)	Max PGA (g) for Strike-slip (M6.82)
1,300	0.611467	0.545632
4,500	0.515322	0.460025
20,000	0.30063	0.278629
100,000	0.182092	0.146067

Table 5. Maximum Peak Ground Acceleration (PGA) (g) for **Reverse-slip motion** on the Meers Fault with a **dip of 70° and a recurrence interval of 4,500 yrs**.

Rake	Max PGA (g) for Reverse/Thrust (M7.11)	Max PGA (g) for Reverse/Thrust (M6.80)
30.0°	0.578748	0.474928
11.0°	0.551526	0.457121

Table 6. Maximum Peak Ground Acceleration (PGA) (g) for **Reverse-slip motion** on the Meers Fault with a **dip of 55° and a recurrence interval of 4,500 yrs**.

Rake	Max PGA (g) for Reverse/Thrust (M7.11)	Max PGA (g) for Reverse/Thrust (M6.80)
30.0°	0.559473	0.450493
11.0°	0.551049	0.44023

6. Discussion and Conclusions

The percent difference for the recurrence interval maximum PGA values shows a larger change than the percent difference for the rupture length or magnitude values. This is evident by comparing the distribution of PGA values on the maps (Figure 2). The distribution and values change more drastically along the recurrence interval axis as compared to the rupture length axis. Although the rupture length or magnitude has an effect on the PGA, the recurrence interval is shown to have a more dramatic effect. Although there was a slight change, the rake and dip have the least effect on the PGA distribution and values. Overall, the largest factor and therefore the largest uncertainty in the probabilistic seismic hazard assessment was the change in recurrence interval. Since the resulting calculated ground motions are self-consistent and change as would be expected given a specific parameter like recurrence interval. The number of iterations was not considered an issue for this study.

In 2008, the USGS published an open-file report on the National Seismic Hazards (NSH) associated with potentially hazardous faults within the United States (Peterson et al., 2008, revision II). In the report, PGA values were calculated for the lower 48 conterminous states and the Central and Eastern United States (CEUS), which include the Meers fault (Figure 4). The parameters used are similar to the parameters presented within this study (Tables 7 and 8). Using a recurrence interval of 4,500 years and a magnitude of 7.0, the maximum PGA value for the USGS hazards assessment of the Meers fault is 0.21334 (Peterson et al., 2008, revision II). The approximately 50% lower PGA values could be due to the slight differences in parameters and the different attenuation models used in the USGS study.

United States Geological Survey
 Peak Ground Acceleration
 with 2%/50 yr, 2008

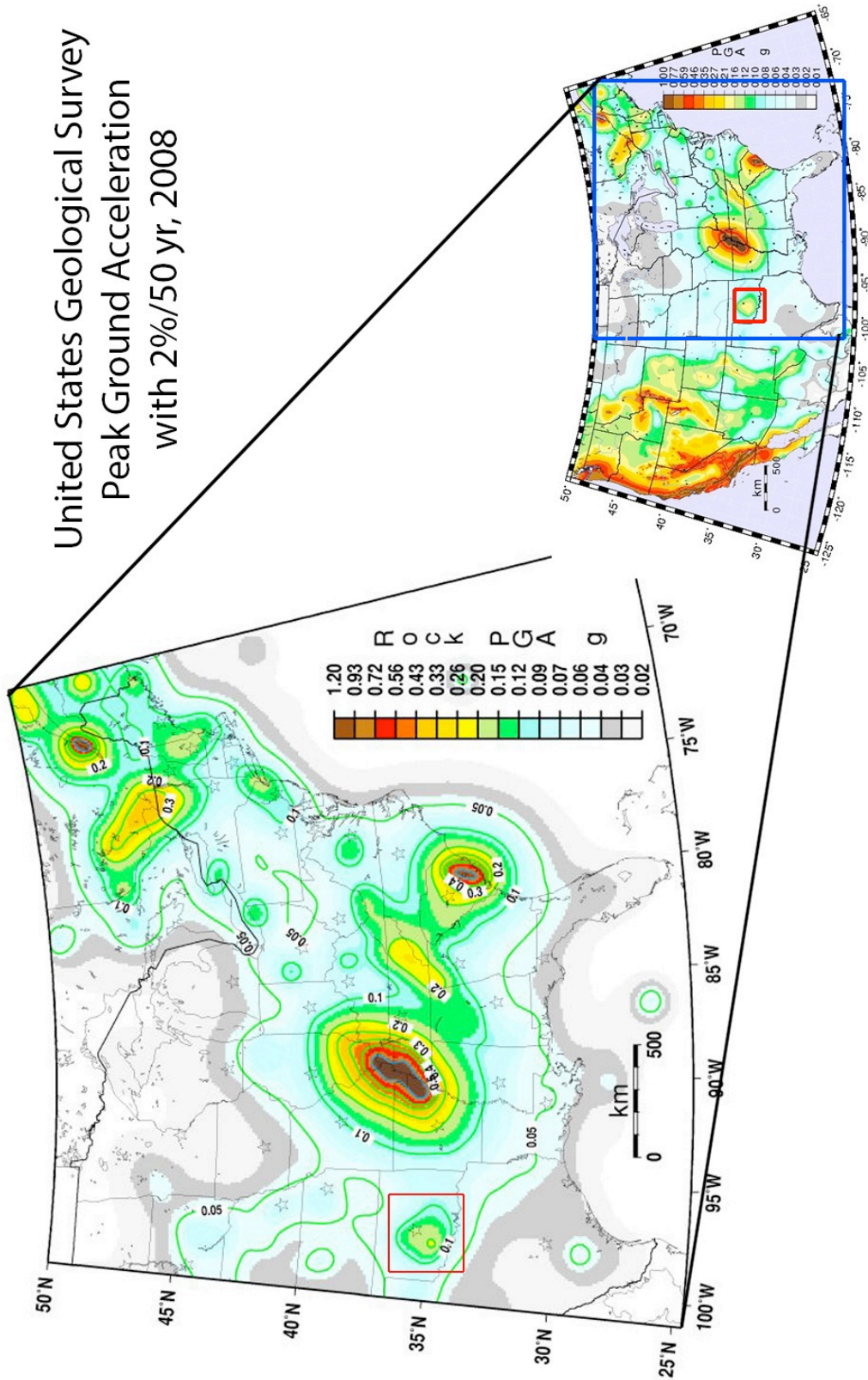


Figure 4. Peak Ground Acceleration (PGA) maps for the lower 48 conterminous states and the CEUS conducted by the USGS published in 2008 in standard gravity (g). The recurrence interval used was 4,500 years for the Meers fault with a 2% probability of exceedance (POE) in an investigation time of 50 years. A red box surrounds the Meers fault PGA portion of the map (modified from Peterson et al., 2008, revision II).

The Meers fault remains the largest visible surface expression with known Holocene offset and represents the largest known seismic hazard over a broad region in the Central United States. The sensitivity analysis to PSHA input parameters for the Meers fault clearly demonstrates that recurrence interval most dramatically affects the associated seismic hazard. Other input parameters affect the calculated hazard but none to the extent of the recurrence interval. Published recurrence interval estimates for the Meers Fault range from 1,300 to 100,000 years; further research to quantify possible recurrence intervals and their uncertainties would improve PSHA calculations for the Meers fault and reduce the uncertainty in seismic hazard estimates.

Table 7. Some of the Meers fault PGA parameters for the hazards assessment by the USGS in 2008 (Peterson et al., 2008, revision II).

Parameter	Value(s)
Sense of Slip	Strike-slip
Characteristic Moment Magnitude	7.0
Rupture Length	35 km
Dip	89° SW
Rake	0°
Recurrence Interval	4,500 years
POE	0.02
Investigation Time	50 years
Site Type	Uniform Firm Rock
Upper Seismogenic Depth	0 km
Lower Seismogenic Depth	15 km
Distance from source	Up to 1,000 km

Table 8. Attenuation models used in the CEUS hazards assessment by the USGS in 2008 (taken from Peterson et al., 2008, revision II).

Single corner—finite fault	Weight
Toro and others (1997)	0.2
Silva and others (2002)—constant stress drop w/ saturation	0.1
Single corner—point source with Moho bounce	
Frankel and others (1996)	0.1
Dynamic corner frequency	
Atkinson and Boore (2006) 140 bar stress drop	0.1
Atkinson and Boore (2006) 200 bar stress drop	0.1
Full waveform simulation	
Somerville and others (2001) for large earthquakes	0.2
Hybrid empirical model	
Campbell (2003)	0.1
Tavakoli and Pezeshk (2005)	0.1

7. Acknowledgements

We would like to thank Dr. Kenneth Luza for his careful review of this report. We would also like to thank Dr. Randy Keller for his input and guidance. This project was funded in part by a grant titled "Earthquake State Assistance Cooperative Agreement" from the National Earthquake Hazards Reduction Program (NEHRP) through the U.S. Department of Homeland Security and the Oklahoma Office of Emergency Management.

8. References

- Abrahamson, N. A., and Silva, W. J., 2008, Summary of the Abrahamson & Silva NGA ground-motion relations: *Earthquake Spectra*, v. 24, no. 1, p. 67-97.
- Boore, D.M., and Atkinson, G.M., 2008, Ground-motion prediction equations for the average horizontal component of PGA, PGV, and 5%-Damped PSA at spectral periods between 0.01s and 10.0s: *Earthquake Spectra*, v. 24, no 1, p. 99-138.
- Campbell, K. W. and Bozorgnia, Y., 2008, NGA ground motion model for the geometric mean horizontal component of PGA, PGV, PGD and 5% damped linear elastic response spectra for periods ranging from 0.01 to 10s: *Earthquake Spectra*, v. 24, no. 1, p. 139-171.
- Chiou, B. S.-J., and Youngs, R. R., 2008, An NGA model for the average horizontal component of peak ground motion and response spectra: *Earthquake Spectra*, v. 24, no. 1, p. 173-215.
- Crone, A. J., and Luza, K. V., 1990, Style and timing of Holocene surface faulting on the Meers fault, southwestern Oklahoma: *Geological Society of America Bulletin*, v. 102, p. 1-17.
- Crowley, H., Monelli, D., Pagani, M., Silva, V., and Weatherill, G., 2012, *OpenQuake User's Manual*: openquake.org, no. 1.1, 130 p.
- Field, E. H., Jordan, T. H., and Cornell, C. A., 2003, OpenSSA: A developing community-modeling environment for seismic hazard analysis: *Seismological Research Letter*, v. 74, no. 4, p. 406-419.
- Gutenberg, B., and Richter, C.F., 1944, Frequency of earthquakes in California: *Seismological Society of America Bulletin*, v. 34, p. 185-188.
- Ham, W. E., Denison, R. E., and Merritt, C. A., 1964, Basement rocks and structural evolution of southwestern Oklahoma: *Oklahoma Geological Survey Bulletin*, v. 95, 302 p.
- Harlton, B. H., 1963, Frontal Wichita fault system of southwestern Oklahoma: *American Association Petroleum Geologists Bulletin*, v. 47, p. 1552-1580.
- Hermann, R.B., Benz, H. and Ammon, C.J., 2011, Monitoring the earthquake source process in North America: *Seismological Society of America Bulletin*, v. 101, p. 2609-2625.
- Holland, A. A., Toth, C. R., and Baker, E. M., 2013, Probabilistic seismic hazard assessment and observed ground motions for the Arcadia, Oklahoma, dam site: *Oklahoma Geological Survey Special Publication*, SP2013-01, 72 p.
- Jones-Cecil, M., 1995, Structural controls of Holocene reactivation of the Meers fault, southwestern, Oklahoma, from magnetic studies: *Geological Society of America Bulletin*, v. 107, p. 98-112.
- Kelson, K. I., and Swan, F. H., 1990, Paleoseismic history of the Meers fault, Southwestern Oklahoma, and implications for evaluations of earthquake Hazards in the central and eastern United States: Unpublished Report, 25 p.
- Lemiscki, P. J. and Brown, L. D., 1988, Variable crustal structure of strike-slip fault zones as observed on deep seismic reflection profiles: *Geological Society of America Bulletin*, v. 100, p. 665-676.
- Luza, K. V., Madole, R. F., and Crone, A. J., 1987, Investigation of the Meers fault, Southwestern, Oklahoma: *Oklahoma Geological Survey Special Publication*, v. 87-1, 75 p.
- Madole, R. F., 1988, Stratigraphic evidence of Holocene faulting in the mid-continent: The Meers fault, southwestern Oklahoma: *Geological Society of America Bulletin*, v. 100, p. 392-401.

- Peterson, M.D., Frankel, A.D., Harmsen, S.C., Mueller, C.S., Haller, K.M., Wheller, R.L., Wesson, R.L., Zeng, Y., Boyd, O.S., Perkins, D.M., Luco, N., Field, E.H., Wills, C.J., and Rustales, K.S., 2008, Documentation for the 2008 update to the United States national seismic hazard maps: USGS 128 p.
- Ramelli, A. K., and Slemmons, D. B., 1986, Neotectonic activity of the Meers fault: Oklahoma Geological Survey Guidebook, v. 24, p. 45-54.
- Sadigh, K., Chang, C. Y., Egan, J. A., Makdisi, F., and Youngs, R. R., 1997, Attenuation relationships for shallow crustal earthquakes based on California strong motion data: Seismological Research Letters, v. 68, no. 1, p. 180-189.
- Slemmons, D. B., Ramelli, A. K., and Brocoum, S., 1980, Earthquake potential of the Meers fault, Oklahoma: Seismological Society of America Annual Meeting Abstracts, v. 80.
- USGS, 1994, Rault number 1031b, Meers fault, in Quaternary fault and fold database of the United States, *in* Crone, A. J., ed.: <http://earthquakes.usgs.gov/regional/qfaults>.
- Wells, D. L., and Coppersmith, K. J., 1994, New empirical relationships among magnitude, rupture length, rupture width, rupture area, and surface displacement: Seismological Society of America Bulletin, v. 84, no. 4, p. 974-1022.
- Zoback, M.L., and Zoback, M.D., 1980, State of stress in the conterminous United States: Journal of Geophysical Research, v. 86, p. 6113-6156.